A New Similarity Measure for Non-local Means Denoising

Bin Cai[1,2], Wei Liu[1], Zhong Zheng[1], and Zeng-Fu Wang[1,2(✉)]

[1] Institute of Intelligent Machines, Chinese Academy of Sciences, Hefei 230031, Anhui, China
zfwang@ustc.edu.cn
[2] School of Information Science and Technology,
University of Science and Technology of China, Hefei 230027, Anhui, China

Abstract. Non-local means (NLM) denoising algorithm is a good similarity measure based denoising algorithm for images with repetitive textures. However, NLM cannot handle the large rotation. In this paper, we propose a rotation-invariant and noise-resistant similarity measure based on improved LBP operator, and use it to search for similar image patches. In addition, in order to speed up the algorithm, an automatic selection strategy of similar patches is proposed. Consequently, the self-similarity can be used to obtain more similar patches for denoising. Experiment results demonstrate that the proposed method achieved higher peak signal-to-noise ratio (PSNR) and more visual pleasing results than some state-of-art methods.

Keywords: Rotation-invariant · Similarity measure · NLM · PSNR

1 Introduction

The goal of image denoising methods is to recover the original image from a noisy measurement. Several methods have been proposed to remove the noise and recover the true image. Most of them can be divided into two parts, spatial filtering algorithm and transform domain filtering algorithm. The former mainly includes the mean filtering, median filtering, wiener filtering and non-local means (NLM) filtering, etc [1-3]. The latter mainly includes wavelet threshold filtering [4-6], and filtering method based on dictionary learning [7-9], etc. The NLM [3] algorithm extends the local calculation model to non-local and it has been proved to have better performance than other classic denoising algorithm. This denoising filter searches similar patches and uses them in a weighted average, which the weights depend on the amount of similarity. So, the similarity measurement between patches is the most important part in NLM denoising algorithm.

In order to obtain better filtering performance, many researchers have conducted the thorough research on the basis of NLM [10-15]. By sparse 3D transform-domain collaborative filtering, the BM3D algorithm obtains very good filtering effect. For the research on the speed of operation, researchers mainly use the pre-selection method [16-17]. Although these methods in a certain extent, improve the filtering performance, there are still some shortcomings. Most improved filtering algorithms cannot handle rotation or mirroring.

H. Zha et al. (Eds.): CCCV 2015, Part I, CCIS 546, pp. 306–316, 2015.
DOI: 10.1007/978-3-662-48558-3_31

Local binary pattern (LBP) operator was proposed by Ojala et al. [18]. Although it can capture the very local structure of the texture, the original LBP codes are sensitive to noise and image rotation. Therefore, we propose an improved LBP operator, and put forward an improved method for searching for similar image patches on the basis of the improved LBP operator. The improved similarity measure methods are as follows. Given a pixel i, $N(i)$ denotes a square neighborhood of fixed size and centered at pixel i, $N(j)$ centered at pixel j is the neighborhood of patch $N(i)$. We obtain $N^{'}(i)$, $N^{'}(j)$ by rotating $N(i)$ and $N(j)$ which based on the improved LBP operator of pixel i and j. Then the distance between $N^{'}(i)$ and $N^{'}(j)$ is defined as the similarity measurement of pixel i and j. And in order to obtain the most suitable similar patches and speed up the algorithm, we propose an automatic selection method. As the improved similarity measure can better reflect the similarity between image patches, the proposed algorithm can remove noise more effectively while preserving the image details.

2 NLM Algorithm

Given a noisy image $g = \{g(i) \mid i \in \Omega\}$, where Ω represents the image area, the filtered image $\hat{f}$ at the point i is then computed by

$$\hat{f}(i) = \frac{\sum_{j \in I} w(i,j) g(j)}{\sum_{j \in I} w(i,j)} \tag{1}$$

$$w(i,j) = \exp\left(-\frac{d(i,j)}{h^2}\right) \tag{2}$$

$$d(i,j) = \| N(i) - N(j) \|_{2,a}^2 \tag{3}$$

Where a is the standard deviation of the Gauss function, $d(i,j)$ is the distance between patches, I is the neighborhood pixel of pixel i. And the family of weights $w(i,j)$ depend on the similarity between the pixels i and j.

The NLM algorithm not only compares the difference between the gray values of the pixels, but also considers the redundancy in the image structure. However, it is not invariant under any transformation such as rotations or mirroring. So, it did not make full use of the self similarity of the image information.

3 Improved NLM Algorithm

In this section we propose an improved block matching algorithm which is invariant under rotation and mirroring. First, An improved LBP operator will be introduced. Then we will show how it works for our improved block matching algorithm. Finally, we will analysis how our proposed improved NLM algorithm works.

3.1 Improved LBP Operator

The original LBP[18] is a gray-scale texture operator. Given a central pixel g_c, a pattern number is computed by comparing its value with those of its neighborhoods:

$$LBP_{R,P} = \sum_{p=0}^{P-1} s(g_p - g_c)2^p \tag{4}$$

Where $s(x) = \begin{cases} 1, x \geq 0 \\ 0, x < 0 \end{cases}$, g_p is the neighbor of g_c. P is the sample number of g_p, R is the radius of the neighborhood. As the original LBP operator can capture the very local structure of texture, it is widely used texture classification, face recognition and so on. So, this ability just can be applied to NLM algorithm. As the original LBP operator is sensitive to noise and rotation, we propose an improved LBP operator $ILBP_{R,P}^{ri}$:

$$ILBP_{R,P}^{ri} = \min\{ROR(LBPM_{R,P}, k), k = 0, \cdots, P-1\} \tag{5}$$

$$LBPM_{R,P} = \sum_{p=0}^{P-1} s(\overline{g_p} - \overline{g_c})2^p \tag{6}$$

Where $\overline{g_c}$ is the means of g_c and its 8-connected. $\overline{g_p}$ is the means of g_p and its 4-connected (see in Fig. 1). Due to this strategy, the $LBPM_{R,P}$ is robust to noise , it can also keep the difference between the neighborhood points even the radius is small($R=1$). $ROR(\bullet, k)$ [18]performs a circular k-step bit-wise right shift on $LBPM_{R,P}$, so, the $ILBP_{R,P}^{ri}$ is rotation-invariant.

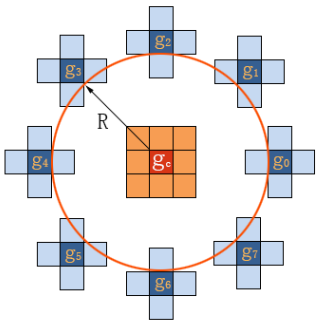

Fig. 1. The (R,P) neighborhood type used to $LBPM_{R,P}$ operator: central pixel and its $P=8$ neighbors on circle of radius R.

3.2 Rotation-Invariant and Noise-Resistant Similarity Measurement

There are many similar structures in natural images. In order to determine the similarity between two pixels, the standard block matching method of NLM usually compares the gray value between the corresponding position of each patch. However, there are not only the original block translation results, more is rotated by the original block. If we use the standard block matching method, many similar patch has not been able to find, and this will diminish the contributions of these similar structure to suppress noise.

Based on the above analysis, we propose an improved similarity measure method. The new one can make better use of the redundant information, thus we can obtain a better filtering effect. Here are the details.

Suppose the size of $N(i)$ and $N(j)$ is $(2R+1)\times(2R+1)$. We can obtain $ILBP^{ri}_{R,P}$ of pixel i and j with radius R , neighborhood sample points $P=8$ using Eq. (5), Eq.(6). We can also obtain the circular step k_i bit-wise right shift from $LBPM_{R,P}$ to $ILBP^{ri}_{R,P}$ of pixel i, and the circular step k_j bit-wise right shift from $LBPM_{R,P}$ to $ILBP^{ri}_{R,P}$ of pixel j. So, the rotated patch $N'(i)$ from $N(i)$ is then computed by

$$\begin{aligned} \boldsymbol{N(i)} &= \{\boldsymbol{x}_{r,8r}, \boldsymbol{r}=0,\cdots,\boldsymbol{R}\} \\ &= \{[\boldsymbol{x}_{r,8r,0},\cdots,\boldsymbol{x}_{r,8r,k_i-1},\boldsymbol{x}_{r,8r,k_i},\cdots,\boldsymbol{x}_{r,8r,8r-1}]^T\} \end{aligned} \tag{7}$$

$$\begin{aligned} \boldsymbol{N'(i)} &= \{\boldsymbol{x}'_{r,8r}, \boldsymbol{r}=0,\cdots,\boldsymbol{R}\} \\ &= \{[\boldsymbol{x}_{r,8r,k_i},\cdots,\boldsymbol{x}_{r,8r,8r-1},\boldsymbol{x}_{r,8r,0},\cdots,\boldsymbol{x}_{r,8r,k_i-1}]^T\} \end{aligned} \tag{8}$$

Where $\boldsymbol{x}_{r,8r}$ are the neighbors of pixel i on radius r, and $\boldsymbol{x}'_{r,8r}$ is the result by a circular k_i step bit-wise right shift from $\boldsymbol{x}_{r,8r}$ (see in Fig. 2). We can also obtain $N'(j)$ rotated from $N(j)$ using the same strategy.

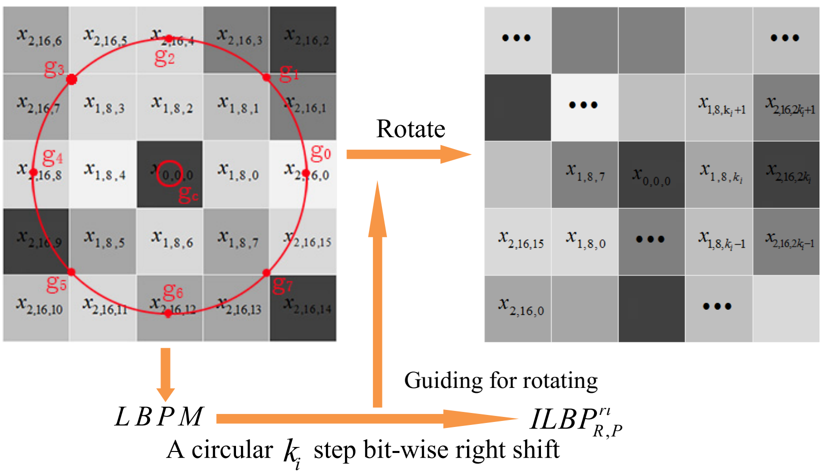

Fig. 2. Illustration of patch rotation

Let d_1 be the distance between $N'(i)$ and $N'(j)$. So, the similarity of the pixel i and j can be measured by distance d_1.

$$d_1 = \| N'(i) - N'(j) \|_{2,a}^2 \tag{9}$$

Fig. 3 shows the advantage in finding similar pixels using our new similarity measure method. We can see, for a given sample point (red box), our improved similarity measure method can still accurately find more similar pixels even in the noise environment.

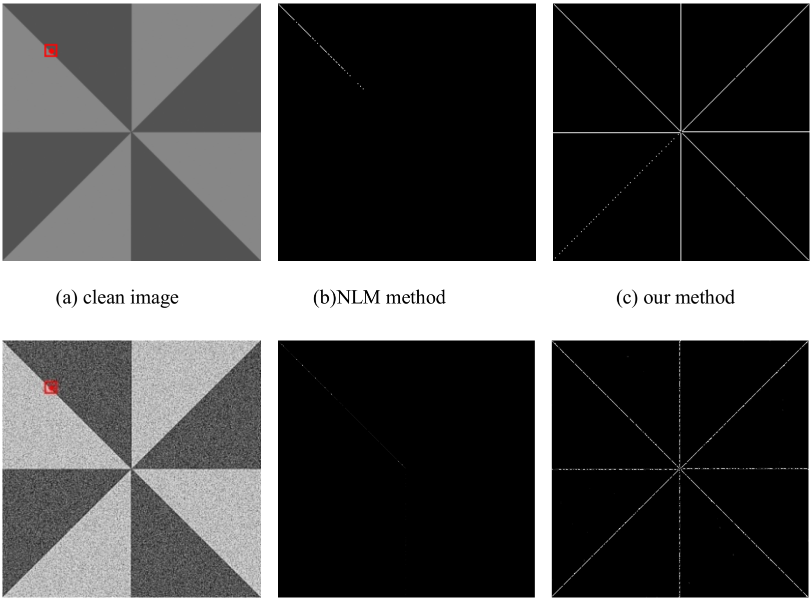

(a) clean image (b)NLM method (c) our method

(d)noisy image (e)NLM method (f)our method

Fig. 3. Similar pixels of the sample point

3.3 Automatic Selection of Similar Sets

For a given pixel i, we put the distances between $N(i)$ and all its neighbor patches $N(j)$ into vector $\mathbf{v} = (d_{i,j} \mid j = 1, \cdots, n)$ using Eq. (9). If we take all the distance in $\mathbf{v}$ for the weighted average, there will be high complexity. And the dissimilar patches for the weighted average will reduce the denoising performance. So we propose an automatic selection of the similar sets. First, the distances $d_{i,j}$ in $\mathbf{v}$ are sorted in non-descending order, denoted as $\hat{\mathbf{v}} = (d_{i,j}(k) \mid k = 1, \cdots, n)$, k is the sequence number of $d_{i,j}$ in $\hat{\mathbf{v}}$. Second, we divide $\hat{\mathbf{v}}$ into L segments (in experiment $L = 10$), and get the mean value of each segment into vector $\overline{\mathbf{v}}$.

$$\bar{\mathbf{v}} = (\bar{d}_l \mid \bar{d}_l = \frac{1}{L_1} \sum_{k=(l-1)\cdot L_1 + 1}^{l \cdot L_1} d_{i,j}(k), l = 1, \cdots, L) \tag{10}$$

where $L_1 = {n}/{L}$, and n is the number of pixels in the neighborhood of i. Third, we find the maximum gradient of $\bar{d}_l$ in vector $\bar{\mathbf{v}}$ as follows:

$$grad_M = \max(g_l \mid g_l = \bar{d}_{l+1} - \bar{d}_l, l = 1, \cdots, L-1) \tag{11}$$

Where M denotes the position of the maximum gradient. So, the similar sets P can be computed as follows:

$$P = \{N(j) \mid d_{i,j}(k), k = 1, \cdots, M \cdot L_1\} \tag{12}$$

3.4 Modification of the Filter

We want to modify the NLM algorithm using our improved similarity measure instead of the standard patch matching method. By replacing d in Eq. (2) by d_1 in Eq.(9), our improved NLM algorithm is rotationally invariant. And we get the similar patches in Eq. (12) for the weighted average.

Besides, in order to reduce the influence of noise on the similarity calculation, we use the denoised image which is filtered by the original NLM algorithm with smaller parameters as the guiding image for the similarity calculation.

4 Experiments and Discussion

The implementations of our improved NLM algorithm produce competitive results. In our experiments, we add Gaussian white noise of different variance .The test images are show in Fig. 4. Table 1 compares the PSNR [19] and the MSSIM [20] of our improved NLM algorithm, NLM [3], PNLM [14], DDID [21], BM3D [13] and SHIFTABLE-BF [22] for the test images. In all the experimentation we have fixed a search window of 21×21 pixels and a similarity square neighborhood $N(i)$ of 5×5 pixels, and the filtering parameter $h = 10\sigma$ [3].

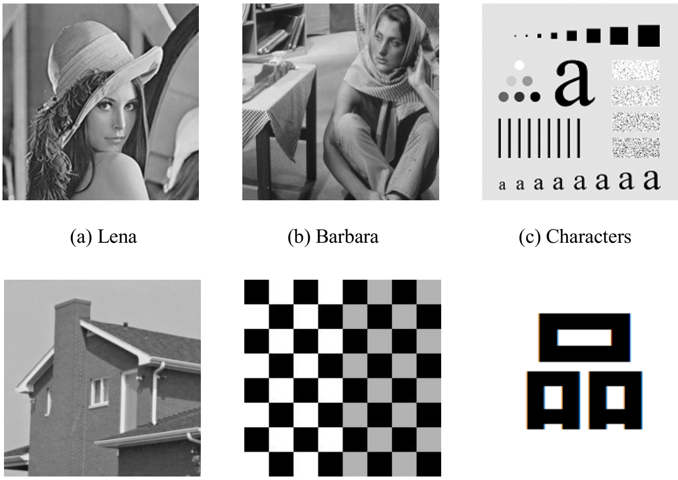

(a) Lena (b) Barbara (c) Characters

(d)House **(e) Checkerboard** **(f) Pin**

Fig. 4. Test image.

As can be seen from Tab.1, compared with the original NLM, our proposed method in comparison with PSNR and MSSIM were significantly improved. And in most cases our proposed method are superior to the selected state of the art method. This shows that, our proposed method can effectively suppress noise and preserve image edge structure information. When the noise standard deviation is large ($\delta = 50, 70$), our proposed method is almost the highest in PSNR and MSSIM compared to NLM, PNLM, SHIFTABLE-BF, DDID, BM3D. For the Checkerboard image with the noise standard deviation $\delta = 70$, the PSNR improvements of our proposed method over BM3D is +4dB. This shows that in case of serious noise pollution, our proposed method has better filtering ability. Especially for the Checkerboard image with the noise standard deviation $\delta = 70$, the MSSIM improvements of our proposed method over the others is +0.1. This shows that in case of serious noise pollution, the proposed algorithm is superior to other methods in the ability to preserve the original structure of the image.

We can see in Fig. 5, 6, the edge of the image filtered by NLM and SHIFTABLE-BF is blurry and lack contrast. And noises still exist in the image filtered by PNLM. The denoising effect of the image filtered by BM3D and DDID is good, but a lot of artificial texture is unnecessarily added. However, the image filtered by our proposed method has better visual effect, and the ringing effect is significantly less than the other methods, the image contrast is higher, homogeneous region is more smooth, besides, the edge and the detail information are preserved better and more clearly. This is mainly because in contrast to the original method, our improved NLM algorithm considers the rotation of the patch, therefore one can find more suitable regions for the weighted average and yield improved results.

Table 1. Performance comparison of different denoising methods (PSNR/MSSIM)

σ		NLM	PNLM	SHIFTABLE-BF	DDID	BM3D	Ours
Lena	30	24.36/ 0.7266	26.92/ 0.7937	24.93/ 0.6948	28.00/ 0.8391	**28.02/ 0.8392**	27.4/ 0.8229
	50	21.46/ 0.6124	24.24/ 0.6682	22.84/ 0.5546	25.05/ 0.7476	25.03/ 0.7394	**25.15/ 0.7576**
	70	19.94/ 0.5361	22.26/ 0.5429	20.77/ 0.4422	23.80/ 0.6875	23.61/ 0.6784	**23.89/ 0.7066**
Barbara	30	23.57/ 0.6625	26.04/ 0.7684	24.41/ 0.6837	**27.26/ 0.8288**	27.12/ 0.8112	26.46/ 0.7838
	50	20.80/ 0.5407	23.48/ 0.6425	22.59/ 0.5766	24.39/ **0.7190**	**24.51**/ 0.7088	24.49/ 0.7103.
	70	19.25/ 0.4609	21.48/ 0.5307	20.59/ 0.4722	21.98/ 0.6084	23.06/ 0.6401	**23.12/ 0.6496**
Character	30	25.65/ 0.8278	26.20/ 0.8521	25.87/ 0.7231	**27.35/ 0.8760**	27.27/ 0.8674	26.60/ 0.8693
	50	20.25/ 0.7285	23.62/ 0.7770	21.03/ 0.5688	24.06/ 0.7838	23.37/ 0.7644	**24.48/ 0.8140**
	70	17.27/ 0.6201	21.39/ 0.6647	18.13/ 0.3840	22.14/ 0.7220	21.66/ 0.7174	**22.75/ 0.7797**
House	30	27.92/ 0.7919	30.44/ 0.7925	27.71/ 0.6389	31.79/ 0.8398	**32.07/ 0.8469**	31.65/ 0.8411
	50	24.67/ 0.7271	27.06/ 0.6637	24.32/ 0.4599	29.24/ 0.7936	29.46/ 0.7995	**29.58/ 0.8129**
	70	22.92/ 0.6723	24.73/ 0.5438	21.73/ 0.3449	27.36/ 0.7521	27.75/ 0.7618	**28.06/ 0.7874**
Checker-board	30	32.15/ 0.9460	31.68/ 0.8730	31.77/ 0.7923	34.66/ 0.9015	36.46/ 0.9577	**39.46/ 0.9738**
	50	25.81/ 0.8808	27.49/ 0.8207	26.54/ 0.6210	29.73/ 0.8482	28.87/ 0.8581	**32.86/ 0.9542**
	70	20.67/ 0.7391	24.11/ 0.7260	21.33/ 0.4572	25.73/ 0.7966	25.97/ 0.8316	**29.97/ 0.9365**
Pin	30	35.93/ 0.9606	33.69/ 0.9133	34.78/ 0.8457	39.03/ 0.9591	**40.77**/ 0.9724	40.54/ **0.9801**
	50	30.53/ 0.9401	30.51/ 0.8846	30.25/ 0.7682	34.63/ 0.9327	32.44/ 0.9243	**36.13/ 0.9645**
	70	23.81/ 0.8771	27.50/ 0.7697	25.44/ 0.7046	31.36/ 0.9046	29.77/ 0.8997	**32.58/ 0.9501**

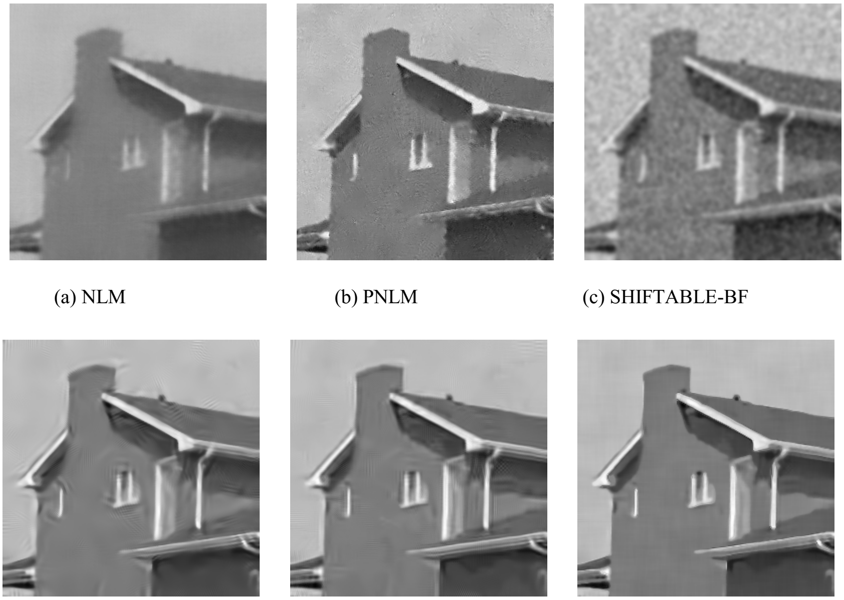

(a) NLM (b) PNLM (c) SHIFTABLE-BF

(d) DDID (e) BM3D (f) Ours

Fig. 5. Comparison of filtering results of House ($\sigma = 50$)

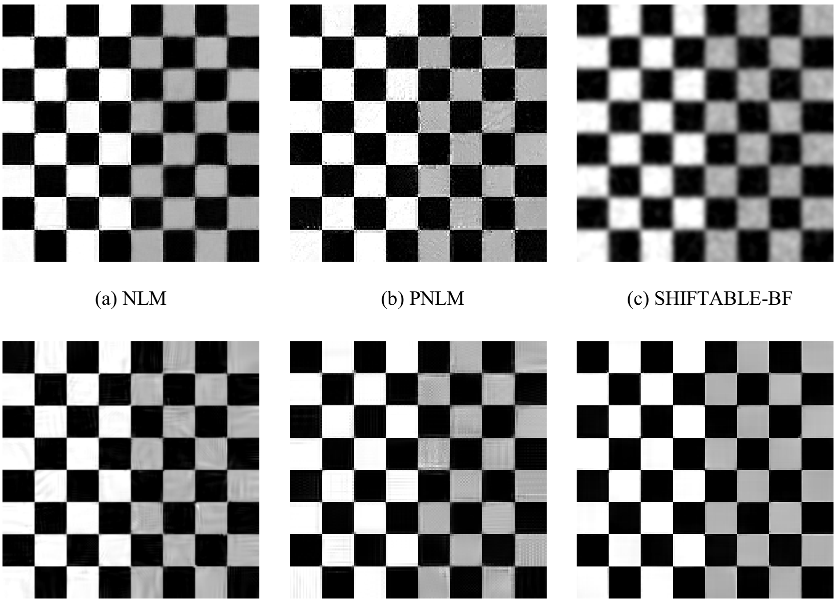

(a) NLM (b) PNLM (c) SHIFTABLE-BF

(d) DDID (e) BM3D (f) Ours

Fig. 6. Comparison of filtering results of Checkerboard ($\sigma = 50$)

5 Conclusion

We have proposed a rotation-invariant and noise-resistant similarity measure that will be used for our improved non-local means algorithm. Before calculating the distance between two patches, the patches are rotated to the same dominant orientation based on the guidance of the improved LBP operator. Moreover, we propose an automatic selection of the similar patches for the weighted average, it helps us get the most suitable similar patches and accelerate the proposed method. Thanks to the similarity measure scheme, our proposed method achieves competitive results with some state-of-the-art methods.

References

1. Huang, H., Lee, T.: Data adaptive median filters for signal and image denoising using a generalized SURE criterion. IEEE Signal Processing Letters **13**(9), 561–564 (2006)
2. Yuan, S., Tan, Y.: Impulse noise removal by a global noise detector and adaptive median filter. Signal Processing. **86**(8), 2123–2128 (2006)
3. Buades, A., Coll, B., Morel, J.: A non-local algorithm for image denoising. In: IEEE Computer Society Conference on Computer Vision and Pattern Recognition, vol. 2, pp. 60-65. San Diego (2005)
4. Sender, L., Selesnick, I.: Bivariate shrinkage functions for wavelet-based denoising exploiting interscale dependency. IEEE Transactions on Signal Processing **20**(11), 2744–2756 (2002)
5. Portilla, J., Strela, V., Wainwright, M.: Image denoising using scale mixtures of Gaussians in the wavelet domain. IEEE Transactions on Image Processing **12**(11), 1338–1351 (2003)
6. Yin, M., Liu, W., Zhao, X.: Image denoising using trivariate prior model in nonsubsampled dual-tree complex contourlet transform domain and non-local means filter in spatial domain. Optik - International Journal for Light and Electron Optics **124**(24), 6896–6904 (2013)
7. Michael, E.: Image denoising via sparse and redundant representations over learned dictionaries. IEEE Transactions on Image Processing **15**(12), 3736–3745 (2006)
8. Chen, G., Xiong, C., Corso, J.: Dictionary transfer for image denoising via domain adaptation. In: Proceedings of IEEE International Conference on Image Processing, pp. 1189-1192 (2012)
9. Sun, D., Gao, Q., Lu, Y.: A novel image denoising algorithm using linear Bayesian MAP estimation based on sparse representation. Signal Processing **100**, 132–145 (2014)
10. Tasdizen, T.: Principal neighborhood dictionaries for nonlocal means image denoising. IEEE Transactions on Image Processing **18**(12), 2649–2660 (2009)
11. Grewenig, S., Zimmer, S., Weickert, J.: Rotationally invariant similarity measures for nonlocal image denoising. Journal of Visual Communication and Image Representation **22**(2), 117–130 (2011)
12. Deledalle, C., Denis, L., Tupin, F.: Iterative weighted maximum likelihood denoising with probabilistic patch-based weights. IEEE Transactions on Image Processing **18**(12), 2661–2672 (2009)
13. Dabov, K., Foi, A., Katkovnik, V.: Image denoising by sparse 3D transform-domain collaborative filtering. IEEE Transactions on Image Processing **16**(8), 2080–2095 (2007)

14. Yue, W., Brian, T., Premkumar, N., Joseph, P.: Probabilistic Non-Local Means. IEEE Signal Processing Letters **20**(8), 763–766 (2013)
15. Deledalle, C., Duval, V., Salmon, J.: Non-Local Methods with Shape-Adaptive Patches (NLM-SAP). Journal of Mathematical Imaging and Vision **43**(2), 103–120 (2012)
16. Mahmoudi, M., Sapiro, G.: Fast image and video denoising via nonlocal means of similar neighborhoods. IEEE Signal Processing Letters **12**(12), 839–842 (2005)
17. Coupé, P., Yger, P., Prima, S.: An optimized blockwise nonlocal means denoising filter for 3-D magnetic images. IEEE Transactions on Medical Imaging **27**(4), 425–441 (2008)
18. Ojala, T., Pietikainen, M., Maenpaa, T.: Multiresolution gray-scale and rotation invariant texture classification with local binary patterns. IEEE Transactions on Pattern Analysis and Machine Intelligence **24**(7), 971–987 (2002)
19. Zhou, W., Bovik, A., Sheikh, H., Simoncelli, E.: Image quality assessment: from error visibility to structural similarity. IEEE Transactions on Image Processing. **13**(4), 600–612 (2004)
20. Alessandroa, F., Vladimir, K., Karen, E.: Pointwise shape adaptive DCT for high quality denoising and deblocking of grayscale and color images. IEEE Transactions on Image Processing. **16**(5), 1395–1411 (2007)
21. Knaus, C., Zwicker, M.: Dual-domain image denoising. In: IEEE International Conference on Image Processing, pp. 440-444 (2013)
22. Chaudhury, K.N.: Acceleration of the shiftable O(1) algorithm for bilateral filtering and non-local means. IEEE Transactions on Image Proc. **22**(4), 1291–1300 (2013)